Proceedings of ASME Turbo Expo 2026
Turbomachinery Technical Conference and Exposition
GT2026
June 15-19, 2026, Milan, Italy

GT2026-176262

DESTRUCTIVE AXIAL VIBRATIONS ON IGC THRUST COLLARS: RCA

Andrea Fusi[1], Andrea Betti[1], Giovanni Karahoxha[1]

[1]Compression Service Technology S.r.l., Florence, Italy

ABSTRACT

This paper presents a case study where axial vibration caused the failure of the first-stage rotor in a three-stage integrally geared centrifugal compressor only a few months after start-up. Inspection of the twin unit revealed the same incipient issue: a series of imprints with variable radial depth caused by direct metal-to-metal rubbing between the collar generator and the impeller.

Axial vibrations in centrifugal compressors are rarely discussed in technical literature. Unlike lateral and torsional vibrations, API 617 [1] has traditionally not required specific design checks for this phenomenon, nor the installation of dedicated monitoring instruments. Only the latest edition mandates axial-vibration monitoring during Mechanical Running Test (MRT) to protect dry gas seals.

The root-cause analysis showed that the thrust collar design was inadequate for this unique configuration. The pinion carried a single large, cantilevered impeller on one end, while the opposite end was free. The combination of gear-tooth geometry, collar design, imbalance-induced synchronous radial vibration, and high axial thrusts generated by the large impeller excited the natural frequency of the axial system. This frequency was too low because of the high mass of the pinion and the insufficient stiffness of the collar. The hydrodynamic oil film (critical for proper collar operation) requires precise geometry that was compromised by these excessive deformations.

An axial vibration probe installed on the free end of the pinion confirmed the presence of axial vibrations with a harmonic spectrum. Several corrective actions were evaluated and, considering the site constraints, the original pinions were replaced, removing the thrust collar and adopting a new design that incorporates an external thrust bearing. After this modification, the issue did not reappear, confirming that the corrective action fully resolved the problem.

Keywords: Integrally Geared Centrifugal Compressor; Axial Vibrations; Thrust Collar; Fracture Mechanics; Fatigue Failure

1. INTRODUCTION

Two identical three-stage Integrally Geared Centrifugal Compressors (IGCs), operating in parallel as Main Air Compressors (MAC A and MAC B), were installed in an Air Separation Unit (ASU) to compress ambient air up to 6 bar(a). Each MAC is driven by an induction motor with an installed power of nearly 9 MW and a rotational speed of 1487 RPM. The first-stage impeller, featuring a semi-open design with 17 blades and a 1000 mm outer diameter, is mounted on the non-drive end of the first pinion, which operates at 7200 RPM. The discharge pressure of the first stage is 2 bar(a). The opposite end of this pinion is free. A second pinion rotates at 9500 RPM and drives the second and third stage impellers installed on the two shaft ends. The large scroll envelope imposes a minimum center distance between the bull gear and the pinions to avoid mechanical interference between adjacent casings. To meet this geometrical constraint while limiting gear peripheral speed, an intermediate idler gear was installed between the bull gear and the second pinion (Fig. 1).

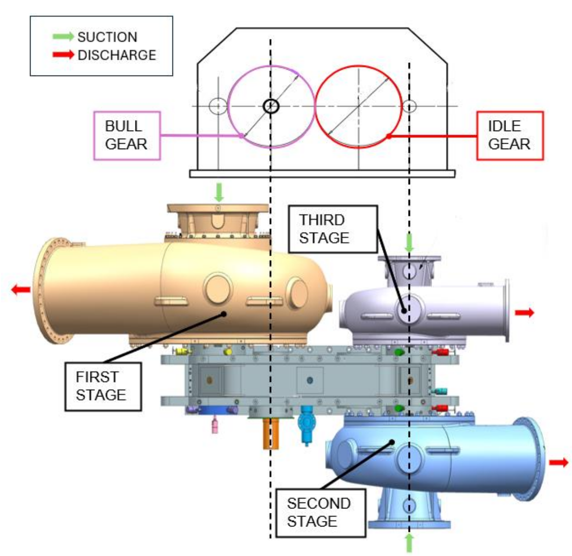

FIGURE 1: GEAR SKETCH AND COMPRESSOR ARRANGEMENT.

In accordance with API 617, the pinions were equipped with X–Y proximity probes located near each journal bearing for lateral vibration monitoring and an axial position probe; on the first pinions the axial probes were installed on the free end.

Both pinions are single helix gear, equipped with thrust collars that transmit the axial loads to the bull gear, which in turn is fitted with a conventional fixed geometry thrust bearing. This solution is typically preferred over installing individual thrust bearings on each pinion because it reduces oil consumption, minimizes footprint, and simplifies maintenance. However, it requires careful management of several mechanical and hydrodynamic challenges by the manufacturer:

- The hydrodynamic support that generates the oil film is created by the rotation of two conical surfaces along their generator lines. These surfaces (Fig. 2) must have a very small angle ($\alpha \approx 1°$), which demands highly accurate geometry and a sufficiently stiff structural arrangement [2].
- For manufacturing reasons, the collar must be shrink-fitted, and the assembly must withstand the stresses generated by axial thrust, shrink-fit interference, and centrifugal forces. The typical design (Fig. 3) consists of a thrust ring axially fixed to a split share ring, held in position by a containment ring.
- Additional attention is required for fatigue stress, as the axial force varies during operation due to the natural rotation of the contact location.

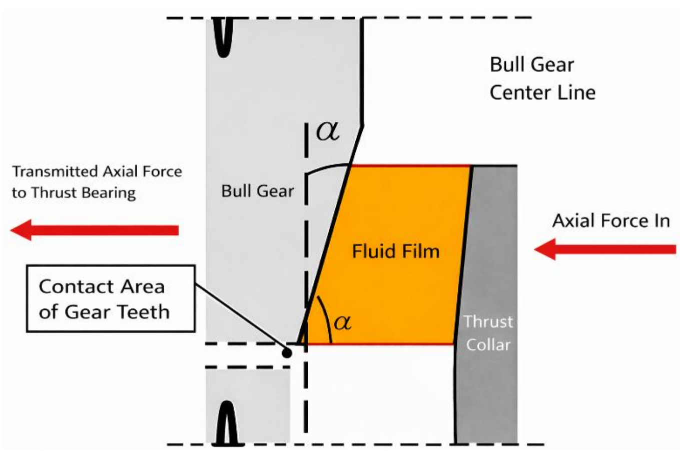

FIGURE 2: THRUST COLLAR WORKING PRINCIPLE.

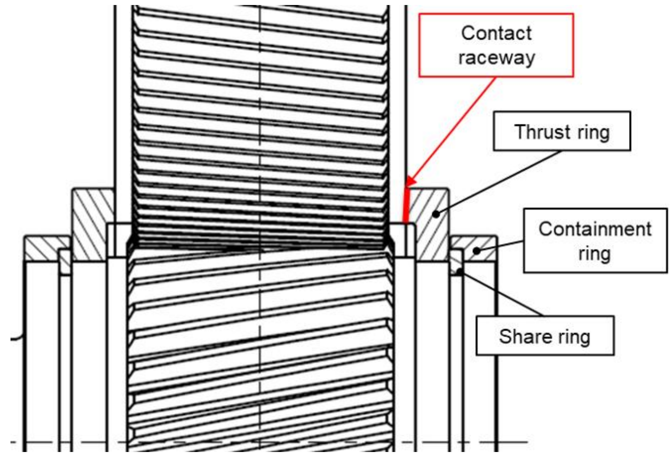

FIGURE 3: THRUST COLLAR ARRANGEMENT.

2. FAILURE

After installation and commissioning, high radial unfiltered vibrations were detected on the first-stage impeller side of both MAC compressors. The situation progressively worsened, eventually leading to destructive events on both MAC A and B, which both triggered Emergency Shut Down (ESD) only a few months after their respective start-up.

During the inspections, in both compressors, the thrust collar ring was found broken into two pieces inside the gear casing, the first-stage rotor shifted axially toward the non-drive end, and the impeller blades rubbed against the stationary components, with an abrasion depth of approximately 11 mm.

In addition, **92 imprints** were observed on the conical surface of the bull gear (MAC A in Fig. 4 and MAC B in Fig. 5). These marks showed variable radial extensions (from about 30% up to 90% of the theoretical contact track) and were clearly caused by direct metal-to-metal rubbing between the bull gear and the thrust collar.

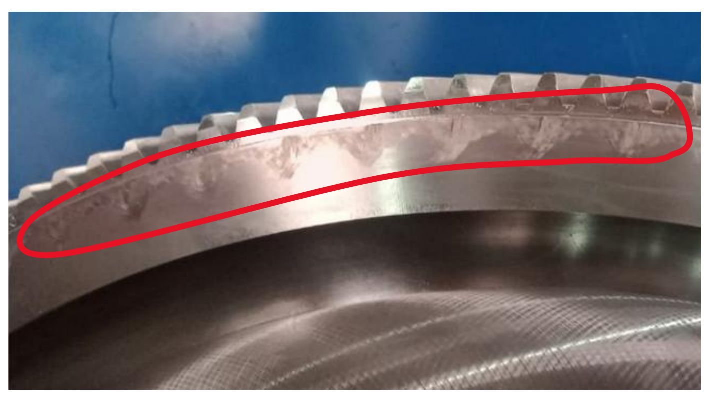

FIGURE 4: 92 IMPRINTS ON MAC A BULL GEAR.

3. ROOT CAUSE ANALYSIS

To explain the periodicity of the imprints, it is important to consider the tooth counts of the bull gear and the first pinion: 184 and 38 teeth, respectively. The marks could not have been generated by a forcing frequency at 92x (2280 Hz), as no such component was detected in the field. Instead, the imprints were generated by a synchronous mechanism imposed by the gear tooth-count interaction. The number of repeatable circumferential contacts (hunting ratio) on the bull gear is:

$$N = \frac{Z_B}{\gcd(Z_B, Z_P)} \quad (1)$$

where Z_B and Z_P are the tooth counts of the bull gear and the first pinion, respectively, and $\gcd(Z_B, Z_P)$ denotes the greatest common divisor of Z_B and Z_P. Since $\gcd(Z_B, Z_P) = 2$, Eq. (1) provides the predicted number of repeatable contact locations, that is N = 92, in agreement with the observed imprint count.

Moreover, MAC B exhibited the same imprint periodicity observed in MAC A, with 92 traces on the bull gear surface. However, in MAC B the imprinting pattern appeared as two distinct, overlapping sets: a first set of 92 traces and a second set, still consisting of 92 traces, circumferentially shifted by approximately one bull-gear tooth pitch (Fig. 5). This behavior indicates that the pinion collar experienced a loss of interference during operation, resulting in collar slippage and a corresponding phase shift of the imprinting locations.

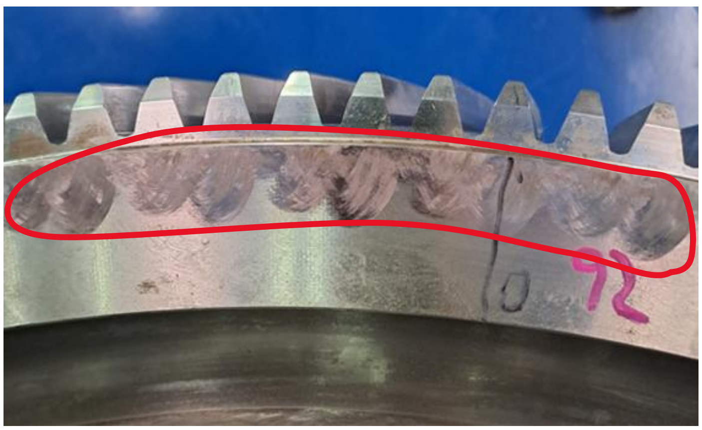

FIGURE 5: 2 SETS OF 92 IMPRINTS ON MAC B BULL GEAR**.**

In MAC B, the shear rings remained in place (Fig. 6), even though the containment ring had slipped approximately 15 mm toward the drive-end side, dragged by the already fractured collar. This slippage was likely caused by a loss of interference in the containment ring.

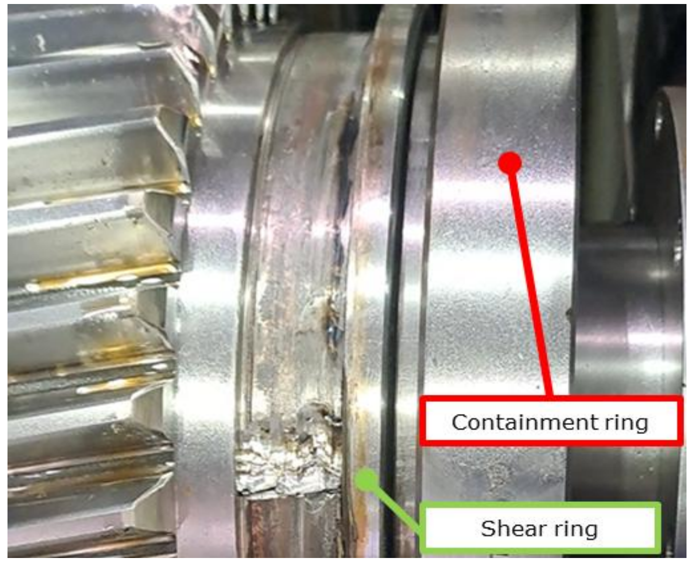

FIGURE 6: MAC B FIRST PINION AS FOUND AFTER ESD.

Because the helicoidal teeth geometry and the thrust collar naturally couple radial synchronous vibration with axial vibration, given the unavoidable imbalance, an axial-vibration resonance emerges as the most credible root cause.

The fractographic examination of the broken thrust collars from both MAC A and B, performed by an accredited laboratory, revealed multiple fatigue cracks originating from the worn surface where the imprints were located (Fig. 7 and Fig. 8).

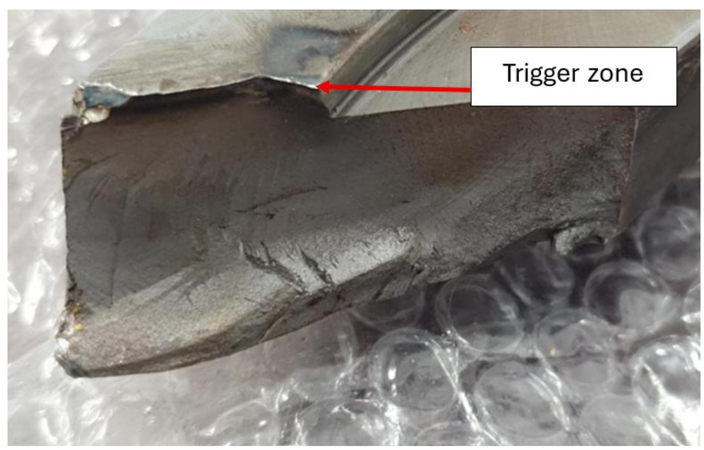

FIGURE 7: MAC A BROKEN RING FRACTURE.

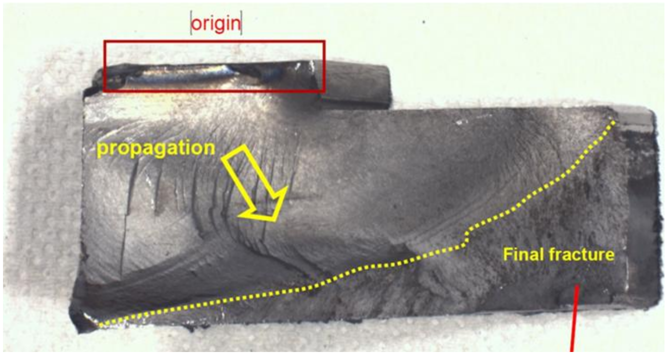

FIGURE 8: MAC A PICTURE FROM FRACTOGRAPHIC EXAMINATION.

The fractures showed all the typical features of fatigue failure—radial marks, beach lines, and a final overload zone—starting a few millimeters from the inner edge of the contact track. The fracture surface also displayed the following characteristics:

- An initial propagation along a radial plane, later transitioning to a surface inclined ≈ 30°.
- Evidence of local heating caused by friction during operation.
- A superficial intergranular fracture zone with deeper transgranular propagation.

Micrographic analysis (Fig. 9) additionally showed alterations in the carburized layer, including the formation of "fresh" martensite (4–5 µm, white layer) and a tempered underlayer (approximately 15 µm, grey layer) with micro-defects. These alterations were attributed to improper grinding during manufacturing; however, they were not considered the root cause of the rapid failure observed in service.

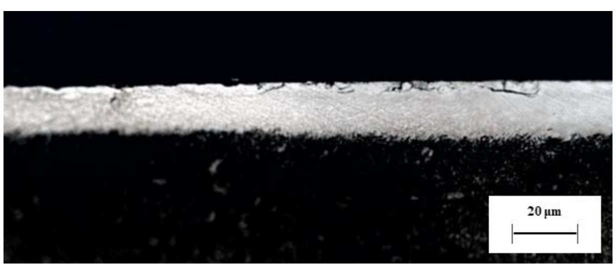

(a) 200X

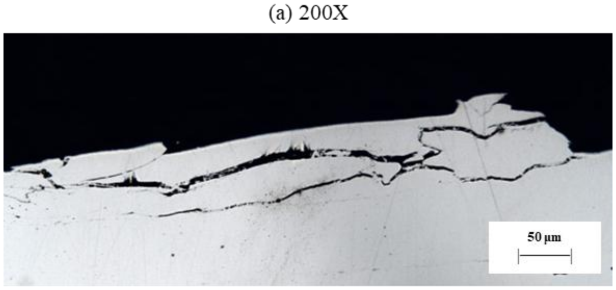

(b) 500X

FIGURE 9: MAC A THRUST COLLAR, PICTURE FROM MICROGRAPHIC EXAMINATION.

The bull gear material also confirmed to be consistent with the manufacturer design and with the state of art of such component: 18CrNiMo7-6 (Rm = 1310 MPa), carburized and tempered in the shaving area, with a surface and a core hardness of 740 and 423 HV respectively [3], and an affected depth of 0.8–1.0 mm.

A closer analysis of the thrust collar operation shows that the theoretical contact on the cone generator does not occur in practice. The deformation of the ring during operation increases the real contact surface beyond the ideal geometric line. The initiation point of the failure (P in Fig. 10) is located a few millimeters from the inner edge of the ring, where the effective contact pressure becomes concentrated due to this deformation.

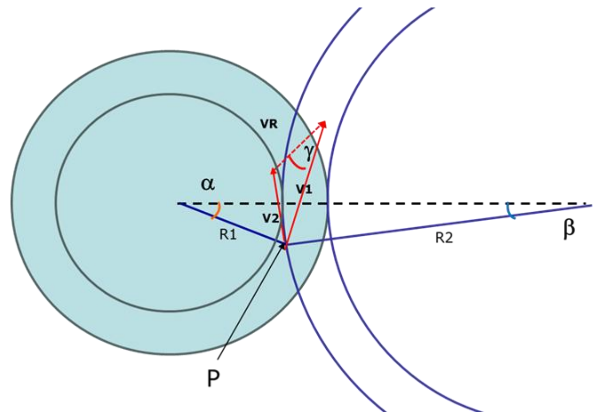

FIGURE 10: THRUST COLLAR CONTACT GEOMETRY.

Considering a location 5 mm from the inner edge, the calculated velocities are: V1 = 99 m/s on the pinion, V2 = 86 m/s on the bull gear, and a relative velocity VR = 31 m/s. This high relative speed, combined with the contact inclination, explains both the presence and the direction of the striations observed on the ring surface. The strong and intermittent nature of the contact stress, together with its orientation, also supports the formation of defects perpendicular to the surface. This behavior is consistent with fretting-type damage mechanisms identified during the fractographic analysis.

External seismic probes detected several vibration components with overall vibration levels between 0.1 and 1 mm/s. Average recorded frequency values are shown in Tab. 1.

TABLE 1: AVERAGE VIBRATION RECORDED

Item	Frequency (Hz)
first-pinion $1x_1$	≈120
second-pinion $1x_2$	≈158
blade-pass $17x_1$	≈2000
blade-pass $17x_2$	≈2700
tooth-mesh $38x_1$	≈4600

At the time of commissioning, axial vibrations were not suspected and therefore were not specifically monitored. Following the ESD event, MAC B was restarted with a spare new rotor and axial-vibration probe installed on the free end of the first pinion to investigate the phenomenon and quantify the axial vibration response under operating conditions. The subsequent analysis showed low radial vibration at the expected frequencies, but **very high axial vibration at multiples of the pinion synchronous frequency—approximately 25 harmonics.** Such spectrums can be seen in Fig. 11, in which only the first 8 harmonics are shown for the sake of visualization.

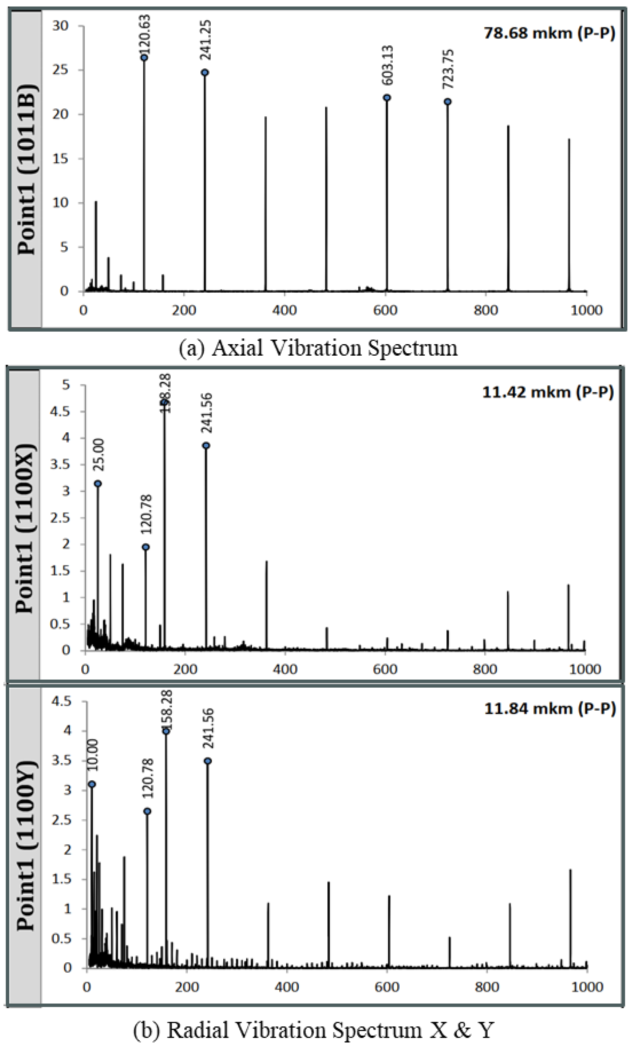

FIGURE 11: MAC B AXIAL AND RADIAL VIBRATION SPECTRUMS.

4. FINITE ELEMENT ANALYSIS

A Finite Element Analysis (FEA) of the thrust ring, performed under static conditions and assuming a reduced contact area between the tapered raceways (due to ring deformation), showed acceptable stress levels. However, the axial deformation of the thrust ring under real operating conditions was found to be high enough to prevent the ideal alignment between the raceways leading to a loss of hydrodynamic support.

Using the worst-case stress values obtained from the FEA, a fatigue assessment was performed according to the Haigh–Goodman method, which resulted in very low safety factors for high-cycle fatigue [4]. Fracture-mechanics calculations [5] [6] further showed that:

- Neither a 10-micron inclusion (typical of industrial-grade materials) nor 50-micron grinding-related surface defects would be sufficient to cause failure unless the actual stresses were far higher than the design values.
- Surface defects of about 100 microns—caused, for example, by friction and local overheating—are large enough to trigger fatigue failure under the measured stress conditions.

The FEA of the pinion was also used to evaluate the stiffness and deformation of the thrust collar. The axial thrust acting on the thrust ring was calculated to be 21 kN. This load was applied to a sector of the ring's circular crown to simulate the Hertzian contact, while also accounting for the diametral interference range and the operating rotational speed (Fig. 12).

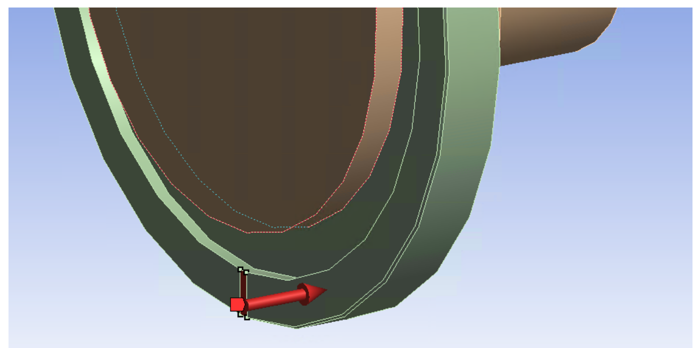

FIGURE 12: APPLIED RING FORCE.

To estimate the natural frequencies of the system, the axial stiffness of the thrust collar was evaluated under the following assumptions:

- The hydrodynamic support of the oil film is absent due to the incorrect geometry created by the ring deformation.
- The stiffness of the bull-gear thrust bearing is much lower than that of the collar and can therefore be assumed as negligible.
- The influence of friction between the gear teeth is negligible.

Under these assumptions, the system can be approximated by a "two-masses, one-spring" model (see Fig. 13).

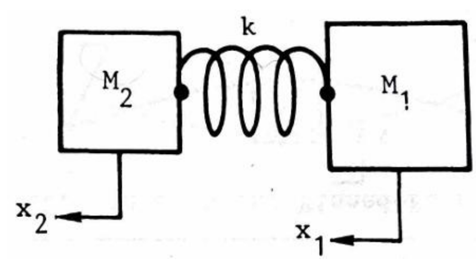

FIGURE 13 - MASS-SPRING MODEL.

Furthermore, by assuming a linear behavior as a first-order approximation, Eq. (2) can be used to estimate the natural frequency value [7]:

$$\omega_i = \frac{1}{2\pi}\left[k\,\frac{M_1 + M_2}{M_1 M_2}\right]^{\frac{1}{2}} \tag{2}$$

where ω_i is the natural system frequency, M_1 and M_2 are the pinion rotor and the bull gear masses, and k is the thrust collar axial stiffness that has been obtained from the FEA as previously mentioned.

Unfortunately, several uncertainties affect this calculation, including:

- The actual non-linear behavior of the ring stiffness.
- The uncertainty of the exact contact location, due to deformation of the ring surface.
- The tolerances associated with the shrink fit.

Each of these factors directly influences the effective axial stiffness of the system and, consequently, the resulting natural frequency. Due to the combined effect of these uncertainties, it is not possible to define a single deterministic value for the axial natural frequency with sufficient confidence.

For this reason, the analysis was carried out by considering a range of plausible stiffness and contact conditions, leading to an estimated axial natural-frequency interval between 95 and 130 Hz. Notably, this interval includes the running-speed excitation at 118.7 Hz ($1x_1$), thereby providing additional support to the hypothesis of resonance amplification.

5. CONCLUSIONS

The stresses predicted under ideal operating conditions alone could not explain the observed failure. In service, the thrust ring deformed, altering the raceway alignment and causing the collapse of the hydrodynamic oil film and consequently its damping capacity, which led to intermittent metal-to-metal contact and imprinting on the bull gear tapered surface.

The first pinion also developed significant axial vibration, coupled with the synchronous radial response. This behavior is consistent with the expected $1x_1$ excitation associated with residual imbalance, which (although compliant with balancing tolerances) cannot be fully eliminated in practice, and with the inherent radial-to-axial coupling introduced by the helical gear tooth contact geometry. Since the running speed (approximately 120 Hz) lies within the estimated axial natural-frequency range of the bull gear–collar–pinion system (95-130 Hz), resonance amplification is considered likely. The resulting increase in alternating stresses reduced the high-cycle fatigue safety margin, ultimately leading to fracture and collapse.

To resolve the issue on site (given the constraints of the installed machines and the lack of space for collar stiffening) the original pinions were replaced and the thrust collar arrangement was removed. The new pinions were redesigned to accommodate an external thrust bearing mounted outside the casing, including a dedicated locating shoulder and an integral thrust face obtained directly from the pinion forging. After this modification, the issue did not reoccur.

For future projects, thrust collars remain a viable solution; however, their design should be primarily driven by deformation (strain) criteria to preserve contact geometry and oil-film stability. In addition, fatigue verification should account for unbalance-driven synchronous excitation and the possibility of axial resonance, since amplified stress oscillations govern the effective fatigue strength.

REFERENCES

[1] API Standard 617: Axial and Centrifugal Compressors and Expander-compressors, 9th Edition, American Petroleum Institute, 2022.

[2] K. Wigant et al., "Tutorial: Rotor-Bearing dynamics of integrally geared turbomachinery," *ATPS - Asia Turbomachinery & Pump Symposium,* 2018.

[3] Y. Shaopeng et al., "Very High Cycle Fatigue Properties of 18CrNiMo7-6 Carburized Steel with Gradient Hardness Distribution.," *Coatings,* vol. 11, 2021.

[4] T. Sakai et al., "Statistical duplex S--N characteristics of high carbon chromium bearing steel in rotating bending in very high cycle regime.," *International Journal of Fatigue,* vol. 32, 2010.

[5] Fracture Mechanics Fundamentals and Applications, Third edition, 2005.

[6] Guide to methods for assessing the acceptability of flows in metallic structures., British Standard BS 7910, 2005.

[7] R. D. Blevins, Formulae for Natural Frequency and Mode Shape, Krieger Pub Co, 2001.